Functional Ecology 2005
19, 202–213

Linking the global carbon cycle to individual metabolism

A. P. ALLEN,*† J. F. GILLOOLY* and J. H. BROWN*‡¶

**Department of Biology, University of New Mexico, Albuquerque, NM 87131, and ‡Santa Fe Institute, 1399 Hyde Park Road, Santa Fe, NM 87501, USA*

Summary

1. We present a model that yields ecosystem-level predictions of the flux, storage and turnover of carbon in three important pools (autotrophs, decomposers, labile soil C) based on the constraints of body size and temperature on individual metabolic rate.
2. The model predicts a 10 000-fold increase in C turnover rates moving from tree- to phytoplankton-dominated ecosystems due to the size dependence of photosynthetic rates.
3. The model predicts a 16-fold increase in rates controlled by respiration (e.g. decomposition, turnover of labile soil C and microbial biomass) over the temperature range 0–30 °C due to the temperature dependence of ATP synthesis in respiratory complexes.
4. The model predicts only a fourfold increase in rates controlled by photosynthesis (e.g. net primary production, litter fall, fine root turnover) over the temperature range 0–30 °C due to the temperature dependence of Rubisco carboxylation in chloroplasts.
5. The difference between the temperature dependence of respiration and photosynthesis yields quantitative predictions for distinct phenomena that include acclimation of plant respiration, geographic gradients in labile C storage, and differences between the short- and long-term temperature dependence of whole-ecosystem CO_2 flux.
6. These four sets of model predictions were tested using global compilations of data on C flux, storage and turnover in ecosystems.
7. Results support the hypothesis that the combined effects of body size and temperature on individual metabolic rate impose important constraints on the global C cycle. The model thus provides a synthetic, mechanistic framework for linking global biogeochemical cycles to cellular-, individual- and community-level processes.

Key-words: acclimation, allometry, global change, labile carbon, metabolic theory

Functional Ecology (2005) **19**, 202–213
doi: 10.1111/j.1365-2435.2005.00952.x

Introduction

The carbon cycle is of major interest in basic and applied ecology (Schlesinger 1997; Schimel *et al*. 2001; Chapin *et al*. 2002). Most biological and human activities are powered by biochemical transformations of C: CO_2 uptake and energy fixation in organic compounds through photosynthesis; and subsequent oxidation of organic compounds and release of energy and CO_2 through respiration and fossil fuel combustion. Over the past three decades our understanding of how biotic and abiotic variables affect ecosystem C dynamics has been advanced by empirical studies, theoretical models and computer simulations. These studies have identified several important variables: temperature, water, light, nutrients and length of growing season (Lieth 1973; Farquhar *et al*. 1980; Vitousek 1984; Raich & Schlesinger 1992; Lloyd & Taylor 1994; Schlesinger 1997; Field *et al*. 1998; Schimel *et al*. 2001; Chapin *et al*. 2002). Ecosystem models often incorporate most or all of these variables into descriptive regressions or process-based simulations to predict C dynamics (Field *et al*. 1998; Schimel *et al*. 2001).

Here we take a different approach. We extend a metabolic theory of ecology (Brown *et al*. 2004) to develop a model that focuses on the role of individual organisms in the global C cycle. This model provides a simple mathematical formulation based on first principles of biology, chemistry and physics. It relates the global C cycle directly to the flux, storage and turnover of C in individual organisms. The model highlights the fundamental influence of two variables – body size and temperature – on C dynamics at all levels of biological organization, from cellular organelles to the biosphere.

The model developed here differs in three important ways from those commonly used in ecosystem ecology. First, it explicitly links the rates of photosynthesis and

†Author to whom correspondence should be addressed. Present address: National Center for Ecological Analysis and Synthesis, Santa Barbara, CA 93101, USA. E-mail: drewa@nceas.ucsb.edu

respiration to the effects of body size and temperature on plant, animal and microbial metabolism. Temperature has long been recognized as an important determinant of C dynamics, but body size has rarely been included in ecosystem models. Second, by quantifying these two primary controls on individual metabolic rate, the model explicitly links ecosystem C cycling to cellular-, individual- and community-level processes. Third, it provides a theoretical baseline for assessing quantitatively the effects of other variables such as water, nutrients and light. Therefore the model provides a simple mechanism-based formulation that complements more complicated empirical and simulation studies of C cycling.

Model assumptions

Like any mathematical model, ours is a deliberate simplification of a complex reality. It aims to capture the essence, but not all the details, of complicated phenomena using mathematical equations. To derive the model, it is necessary to make four simplifying assumptions that are stated and justified as follows.

ASSUMPTION 1

At the level of the organism, C fluxes controlled by photosynthesis and respiration vary predictably with body size and temperature. Specifically, we first assume that C fluxes from individual chloroplasts and respiratory complexes, v, increase predictably with temperature due to the kinetic effects of temperature on rates of photosynthesis and respiration:

$$v = v_o e^{-E/kT} \qquad \text{eqn 1}$$

where $e^{-E/kT}$ is the Boltzmann factor; E is an activation energy that characterizes the exponential effects of temperature on biochemical reaction rates; T is absolute temperature in K; and k is Boltzmann's constant ($8{\cdot}62 \times 10^{-5}$ eV K^{-1}). We next assume that chloroplasts and respiratory complexes are body size-invariant metabolic units with respect to flux, and that the numbers of these units per unit body mass, ρ_i, decline with the increasing body size, M_i, as

$$\rho_i = \rho_o M_i^{-1/4} \qquad \text{eqn 2}$$

The quarter-power scaling exponent on the body size term reflects fundamental constraints on the numbers of metabolic units that can be supplied with energy and materials through fractal-like distribution networks (West *et al*. 1997). Combining equations 1 and 2 yields a general expression for the combined effects of body size and temperature on whole-organism C flux:

$$Q_i = v\rho_i M_i = q_o M_i^{3/4} e^{-E/kT} \qquad \text{eqn 3}$$

where $q_o = v_o\rho_o$ is a normalization constant independent of body size. Equation 3 applies to individual-level C fluxes by autotrophs and heterotrophs. We note, however, that the temperature dependence, characterized by E, differs between photosynthesis and respiration. We note also that using the Boltzmann factor to characterize the temperature dependence of photosynthesis involves approximating a more complex, non-exponential function (see Appendix 1).

ASSUMPTION 2

The flux, storage and turnover of biologically controlled pools of C in ecosystems are controlled by the sum of the metabolic processes of the constituent organisms. Total C storage per unit area, M_{Tot}, for a biomass pool comprised of J individuals in an area of size A is equal to

$$M_{Tot} = (1/A)\sum_{i=1}^{J} M_i = (J/A)\langle M\rangle_J \qquad \text{eqn 4}$$

where $\langle M\rangle_J$ is the average of body size, M_i, for individuals ($= (1/J)\sum_{i=1}^{J} M_i$). Due to mass and energy balance, the C flux per unit area, q, for a biomass pool is equal to the sum of the individual fluxes, Q_i, characterized by equation 3:

$$\begin{aligned} q &= (1/A)\sum_{i=1}^{J} Q_i = (J/A) q_o \langle M^{3/4}\rangle_J e^{-E/kT} \\ &= q_o M_{Tot} \langle M^{-1/4}\rangle_M e^{-E/kT} \propto w \end{aligned} \qquad \text{eqn 5}$$

where $\langle M^{3/4}\rangle_J$ is the average of $M_i^{3/4}$ for individuals ($= (1/J)\sum_{i=1}^{J} M_i^{3/4}$); $\langle M^{-1/4}\rangle_M$ is the average of $M_i^{-1/4}$ for biomass in the pool ($= (1/AM_{Tot})\sum_{i=1}^{J} M_i^{3/4} = \langle M^{3/4}\rangle_J / \langle M\rangle_J$) and w is the supply rate of limiting resources (e.g. water for autotrophs, primary production for heterotrophs) that determine the environment's 'carrying capacity' with respect to individual abundance per unit area, J/A (Enquist *et al*. 1998; Savage *et al*. 2004). Rearranging the terms in equation 5 yields an expression for C turnover in a biomass pool:

$$q/M_{Tot} = q_o(\langle M^{3/4}\rangle_J / \langle M\rangle_J) e^{-E/kT} = q_o \langle M^{-1/4}\rangle_M e^{-E/kT} \qquad \text{eqn 6}$$

In equation 6, q refers specifically to biomass production because C turnover is calculated as the biomass production rate per unit biomass. Equations 1–6 link the flux, storage and turnover of C in ecosystems to the supply rate of limiting resources that determine community abundance, w; the temperature dependence of C transformations in chloroplasts and respiratory complexes, $e^{-E/kT}$; and the size- and temperature-dependence of C fluxes by individual organisms, Q_i.

ASSUMPTION 3

Carbon fluxes in terrestrial ecosystems are due primarily to photosynthesis and respiration. There is abundant evidence that terrestrial C fluxes due to photosynthesis and respiration greatly exceed fluxes due to physical

processes such as precipitation, dry deposition, leaching, runoff and erosion (Schlesinger 1990, 1997; Raich & Schlesinger 1992). For example, C-leaching losses have been estimated as <1% of net primary production (NPP) (Schlesinger 1990).

ASSUMPTION 4

Ecosystems are at steady state over periods of a year or longer, which implies that oxidative metabolism is constrained by gross photosynthesis. This ecosystem-level constraint on oxidative metabolism is consistent with the linear increase of soil respiration with NPP (Raich & Schlesinger 1992), and with studies showing that soil respiration is enhanced by adding reduced C substrates to soils (Gallardo & Schlesinger 1994). Although the steady-state assumption is often violated in nature (Schimel *et al*. 2001), it is useful for three reasons: (i) imbalances are usually small relative to total pool sizes and fluxes; (ii) the mathematical expressions are much simpler because there is no explicit time dependence for rates and states; and, as a consequence, (iii) equilibrial expressions provide a quantitative baseline from which to measure the directions and magnitudes of deviations due to departures from steady-state conditions.

Model derivation

Using assumptions 1–4, we derive a model for C cycling in a simplified terrestrial ecosystem. The derivation entails five steps: (1) identifying C pools and fluxes controlled by biota; (2) characterizing primary production based on the size- and temperature-dependence of photosynthesis by autotrophs; (3) characterizing CO_2 fluxes from autotrophs and hetero-trophs based on the size- and temperature-dependence of respiration; (4) linking soil C dynamics to photosynthesis and respiration; and (5) characterizing ecosystem-level CO_2 flux based on steps 1–5.

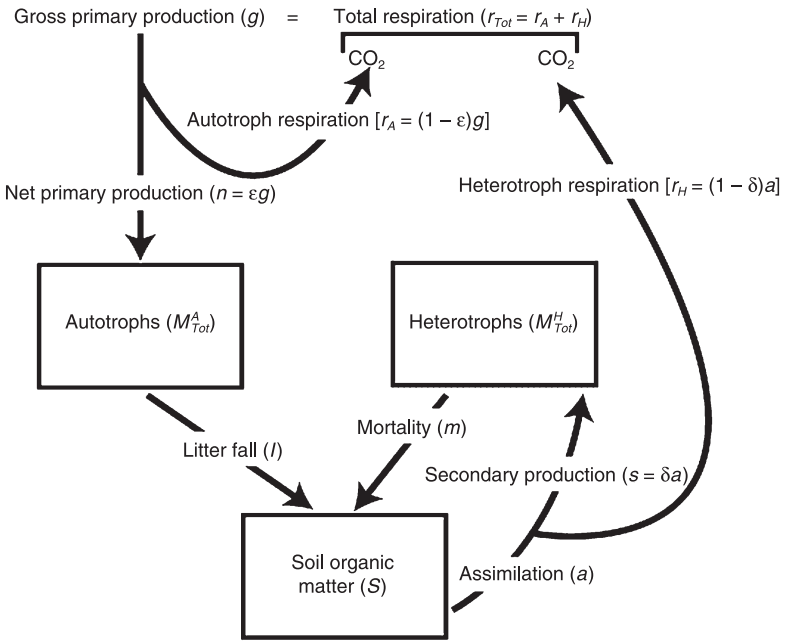

Fig. 1. Important pools (boxes) and fluxes (arrows) in the carbon cycle. At steady state, gross primary production (g) equals total ecosystem respiration (r_{Tot}), and the fraction of r_{Tot} attributable to heterotrophs (r_H) is equal to C-use efficiency by plants ($\varepsilon = r_H/r_{Tot}$).

STEP 1: IDENTIFYING CARBON POOLS AND FLUXES CONTROLLED BY BIOTA

The model considers only C fluxes attributable directly or indirectly to photosynthesis and respiration. It collapses the C cycle down to three biotically controlled pools: autotroph biomass (M^A_{Tot}); heterotroph decomposer biomass (M^H_{Tot}); and non-living labile C in surface litter and soils (S) (Fig. 1); other pools, including herbivores and refractory soil C, are excluded. Herbivores generally consume <20% of the plant biomass produced in terrestrial ecosystems (Schlesinger 1997; Cebrian 1999), and much of the C they consume eventually enters the soil via excretion and biomass production. Refractory C, by definition, cannot be decomposed by soil heterotrophs, and only a small fraction of plant biomass production enters the refractory soil C pool (<1%; Schlesinger 1990, 1997). Refractory C can, however, constitute a large portion of the organic matter stored in soils, because it often accumulates for millennia (Trumbore *et al*. 1996) and is released only by physical processes such as erosion, leaching and fire.

Photosynthesis fuels the global C cycle. At steady state, it constrains the pools and fluxes in Fig. 1 such that gross primary production (GPP), g, equals total ecosystem respiration, r_{Tot}. Our model assumes that fluxes are at steady state over periods of a year or longer, but that short-term imbalances between photosynthate production and consumption can and do occur as a consequence of diurnal and seasonal temperature fluctuations. These imbalances can occur, despite the long-term steady-state assumption, due to storage of labile, reduced C compounds in biomass and soil.

We account for short-term imbalances in the model by time-averaging fluxes on a per hour basis during the entire growing season, denoted by $<>_\tau$. Ecosystem respiration can occur at any time, day or night, when temperatures exceed 0 °C. We therefore define the total length of the growing season, τ, as the number of hours when average daily temperatures exceed 0 °C. The average rate of ecosystem respiration per hour during the growing season (g C m^{-2} h^{-1}) is then calculated by integrating the rate of ecosystem respiration at time t, $r_{Tot}(t)$, over the entire growing season to yield $<r_{Tot}>_\tau = (1/\tau)\int r_{Tot}(t)\mathrm{d}t$. Average GPP per hour is similarly defined as $<g>_\tau = (1/\tau)\int g(t)\mathrm{d}t$. As photosynthesis occurs only during daylight hours, we also express GPP as an average rate per daylight hour in the growing season, $(\tau/\gamma)<g>_\tau$ (g C m^{-2} daylight h^{-1}), where γ is the total number of daylight hours in the growing season, and γ/τ is the average fractional day-length during the growing season.

Having defined time-averaged fluxes, we now trace the fate of C as it moves among the pools in Fig. 1. During the growing season, the average C flux attributable to gross photosynthesis is equal to $\langle g \rangle_\tau$. A fraction ε of this C goes to net primary production of autotroph biomass, $\langle n \rangle_\tau$, where $\langle n \rangle_\tau = \varepsilon \langle g \rangle_\tau$ and $\varepsilon = \langle n \rangle_\tau / \langle g \rangle_\tau$ is the C-use efficiency of plants. The remaining photosynthate is allocated to autotroph respiration [$\langle r_A \rangle_\tau = (1 - \varepsilon)\langle g \rangle_\tau$]. Photosynthate allocated to plant growth is lost from M_{Tot}^A through abscission and death at rate $\langle l \rangle_\tau$. It then enters S, where it is assimilated by heterotrophs at rate $\langle a \rangle_\tau$. A fraction δ of this assimilated C goes to secondary production of heterotroph biomass, $\langle s \rangle_\tau$, where $\langle s \rangle_\tau = \delta \langle a \rangle_\tau$ and $\delta = \langle s \rangle_\tau / \langle a \rangle_\tau$ is the growth efficiency of heterotrophs. The remainder is allocated to heterotroph respiration ($\langle r_H \rangle_\tau = (1 - \delta)\langle a \rangle_\tau$). The C-use efficiency of autotrophs and the growth efficiency of heterotrophs are both approximately independent of temperature ($\varepsilon \approx \delta \approx 0{\cdot}4$) (del Giorgio & Cole 1998; Chapin *et al*. 2002; Gifford 2003).

Steady-state assumptions constrain the time-averaged fluxes in Fig. 1 such that GPP equals total ecosystem respiration by autotrophs and heterotrophs combined:

$$\langle g \rangle_\tau = \langle n \rangle_\tau + \langle r_A \rangle_\tau = \langle r_H \rangle_\tau + \langle r_A \rangle_\tau = \langle r_{Tot} \rangle_\tau \qquad \text{eqn 7}$$

and NPP equals total respiration by heterotrophs:

$$\langle n \rangle_\tau = \langle l \rangle_\tau = \langle r_H \rangle_\tau \qquad \text{eqn 8}$$

Equations 7 and 8 imply that oxidative metabolism is limited by GPP (equation 7), and that heterotroph metabolism is limited by NPP (equation 8). Therefore the fraction of whole-ecosystem respiration attributable to heterotrophs is equal to the C-use efficiency of plants, i.e. $\varepsilon = \langle r_H \rangle_\tau / \langle r_{Tot} \rangle_\tau = \langle n \rangle_\tau / \langle g \rangle_\tau$.

STEP 2: CHARACTERIZING PRIMARY PRODUCTION BASED ON THE SIZE- AND TEMPERATURE-DEPENDENCE OF PHOTOSYNTHESIS

The gross rate of photosynthesis by a plant, P_i (g C daylight h^{-1}), is the product of the rate of photosynthesis per chloroplast, v_{chlo} (g C daylight h^{-1} chloroplast^{-1}), the density of chloroplasts per unit body mass, ρ_i^{chlo} (chloroplasts g^{-1} C), and body mass, M_i (g C) (equation 3). This product yields an expression for the combined effects of body size and temperature on the photosynthetic rate of a plant:

$$P_i = v_{chlo}\rho_i^{chlo} M_i = p_o M_i^{3/4} e^{-E_p/kT} \qquad \text{eqn 9}$$

where $p_o = v_o^{chlo}\rho_o^{chlo}$ is a normalization constant independent of body size and temperature ($g^{1/4}$ C daylight h^{-1}). The size dependence of P_i reflects theory and data indicating that that the density of chloroplasts declines with increasing plant size as $\rho_i^{chlo} = \rho_o^{chlo} M_i^{-1/4}$ (Niklas & Enquist 2001). The temperature dependence is characterized by $v_{chlo} = v_o^{chlo} e^{-E_p/kT}$, where v_o^{chlo} is a normalization parameter (g C chloroplast^{-1} daylight h^{-1}) and E_p is an effective activation energy that characterizes the temperature dependence of photosynthesis (≈0·32 eV). This Boltzmann factor predicts a 3·8-fold increase in the rate of photosynthesis over the temperature range 273–303 K (0–30 °C) ($e^{-E_p/303k}/e^{-E_p/273k} = 3{\cdot}8$) based on the temperature dependence of Rubisco carboxylation in chloroplasts (Appendix 1).

NPP occurs only during daylight hours (g C m^{-2} daylight h^{-1}) and is calculated by summing the photosynthetic fluxes of the plants in the ecosystem (equation 5):

$$n = \varepsilon g = \varepsilon(1/A)\sum_{i=1}^{J} P_i = \varepsilon p_o M_{Tot}^A \langle M_A^{-1/4} \rangle_M e^{-E_p/kT} \qquad \text{eqn 10}$$

where ε is the fraction of photosynthate allocated to primary production of plant biomass (Fig. 1), and $M_{Tot}^A \langle M_A^{-1/4} \rangle_M$ reflects the sizes and abundances of autotrophs per unit area ($g^{3/4}$ C m^{-2}) (equation 5) (Enquist *et al*. 2003). The time-averaged rate of NPP per hour during the growing season (g C m^{-2} h^{-1}) is equal to:

$$\langle n \rangle_\tau = (\gamma/\tau)\varepsilon p_o M_{Tot}^A \langle M_A^{-1/4} \rangle_M \langle e^{-E_p/kT} \rangle_\tau \qquad \text{eqn 11}$$

where $\langle e^{-E_p/kT} \rangle_\tau = (1/\tau)\int e^{-E_p/kT(t)} \mathrm{d}t$, and $T(t)$ is temperature at time t. The term γ/τ in equation 11 is used to express time-averaged NPP on a per hour basis.

STEP 3: CHARACTERIZING CO_2 FLUXES FROM AUTOTROPHS AND HETEROTROPHS BASED ON THE SIZE- AND TEMPERATURE-DEPENDENCE OF INDIVIDUAL RESPIRATION

The respiration rate of an individual, R_i (g C h^{-1}) is the product of the rate of respiration per respiratory complex, v_{resp}; the density of respiratory complexes per unit body mass, ρ_i^{resp}; and body mass M_i (equation 3). This product yields an expression for the combined effects of body size and temperature on the respiration rate of an individual:

$$R_i = v_{resp}\rho_i^{resp} M_i = r_o M_i^{3/4} e^{-E_r/kT} \qquad \text{eqn 12}$$

where $r_o = v_o^{resp}\rho_o^{resp}$ is a normalization parameter ($g^{1/4}$ C h^{-1}) (Gillooly *et al*. 2001). The size dependence of R_i reflects declines in the density of respiratory complexes with increasing body size ($\rho_i^{resp} = \rho_o^{resp} M_i^{-1/4}$) (Else & Hulbert 1985; West *et al*. 2002). The temperature dependence is characterized by the kinetics of ATP synthesis in the respiratory complex ($E_r \approx 0{\cdot}65$ eV) (Ketchum & Nakamoto 1998; Gillooly *et al*. 2001). This Boltzmann factor predicts a 16-fold increase in respiration rate over the temperature range 273–303 K (0–30 °C) ($e^{-E_r/303k}/e^{-E_r/273k} = 16$).

Respiratory fluxes in the ecosystem (g C m^{-2} h^{-1}) are characterized by separately summing the individual respiration rates (equation 5) for autotrophs:

$$r_A = r_o^A M_{Tot}^A <M_A^{-1/4}>_M e^{-E_r/kT} \quad \text{eqn 13}$$

and heterotrophs:

$$r_H = r_o^H M_{Tot}^H <M_H^{-1/4}>_M e^{-E_r/kT} \quad \text{eqn 14}$$

where r_o^A and r_o^H are normalization parameters for individual respiration ($g^{1/4}$ C h^{-1}), and $M_{Tot}^H <M_H^{-1/4}>_M$ reflects the sizes and abundances of heterotrophic decomposers per unit area ($g^{3/4}$ C m^{-2}) (equation 5). Time-averaged fluxes over the growing season, $<r_A>_\tau$ and $<r_H>_\tau$, are calculated as:

$$<r_A>_\tau = r_o^A M_{Tot}^A <M_A^{-1/4}>_M <e^{-E_r/kT}>_\tau \quad \text{eqn 15}$$

and

$$<r_H>_\tau = r_o^H M_{Tot}^H <M_H^{-1/4}>_M <e^{-E_r/kT}>_\tau \quad \text{eqn 16}$$

where $<e^{-E_r/kT}>_\tau = (1/\tau)\int e^{-E_r/kT(t)}dt$ is the average of the Boltzmann factor for the growing season.

An individual's metabolic rate is always equal to its rate of energy acquisition from the environment, but energy acquisition is fuelled by fundamentally different processes for autotrophs (biochemical reduction via photosynthesis) and heterotrophs (biochemical oxidation via respiration). The normalization parameter for heterotroph respiration, r_o^H, is approximately independent of temperature, because energy acquisition and consumption by a heterotroph is fuelled by its own respiration. By contrast, the normalization parameter for plant respiration, r_o^A, must decline with long-term temperature increases because plant respiration is ultimately limited by photosynthate production, which has a weaker temperature dependence ($E_p < E_r$).

We can quantify this commonly observed phenomenon, referred to as respiratory acclimation (Dewar *et al.* 1999), by noting that the time-averaged supply rate of C used for plant respiration is equal to $<g>_\tau - <n>_\tau = (\gamma/\tau)(1-\varepsilon)p_o M_{Tot}^A <M_H^{-1/4}>_M <e^{-E_p/kT}>_\tau$, and that time-averaged C demand for plant respiration is equal to $<r_A>_\tau$ (equation 15). Given our model assumption that total C supply matches total C demand over the growing season, we can equate these two expressions and rearrange terms to yield:

$$r_o^A = (\gamma/\tau)(1-\varepsilon)p_o(<e^{-E_p/kT}>_\tau / <e^{-E_r/kT}>_\tau) \quad \text{eqn 17}$$

In equation 17, fluxes should be averaged over a time scale too short for respiratory acclimation to occur. The parameter r_o^A is insensitive to diurnal temperature fluctuations, but declines in response to temperature increases that are weeks to months long (Dewar *et al.* 1999; Gifford 2003).

Together, equations 13, 15 and 17 predict that the short-term temperature dependence of plant respiration will have an activation energy of E_r, but that the long-term temperature dependence will have an effective activation energy of E_p. Both observations are consistent with experimental data (Dewar *et al.* 1999; Gifford 2003). These equations reconcile differences between the short- and long-term effects of temperature on plant respiration by imposing mass balance on photosynthate production and consumption. Equation 17 also predicts a decline in r_o^A with declines in average day-length, characterized by γ/τ, due to constraints of photosynthate production on plant respiration.

STEP 4: LINKING SOIL CARBON DYNAMICS TO PHOTOSYNTHESIS AND RESPIRATION

The dynamics of labile soil C are characterized by the rate equation:

$$dS/dt = I - (\kappa \cdot S) \quad \text{eqn 18}$$

where I is the rate of C input (g C m^{-2} h^{-1}); and κ is the rate of C loss per unit labile C (h^{-1}) (Jenkinson 1990). The decomposition of organic matter is controlled by heterotroph respiration, r_H, and therefore varies with temperature as:

$$\kappa = r_H/S = k_o e^{-E_r/kT} \quad \text{eqn 19}$$

where κ_o is a normalization parameter, independent of temperature, that reflects the effects of soil texture, water availability and organic matter quality on habitat suitability to decomposers (Jenkinson 1990).

Combining equations 8, 11, 16, 18 and 19 yields the following expressions for the long-term storage of labile C in soil:

$$S = <I>_\tau / <\kappa>_\tau = (\gamma/\tau)(\varepsilon p_o M_A^{Tot} <M_A^{-1/4}>_M / \kappa_o)(<e^{-E_p/kT}>_\tau / <e^{-E_r/kT}>_\tau) \quad \text{eqn 20}$$

and heterotroph biomass:

$$M_{Tot}^H = (\kappa_o / r_o^H <M_H^{-1/4}>_M) S \propto (\gamma/\tau)(<e^{-E_p/kT}>_\tau / <e^{-E_r/kT}>_\tau) \quad \text{eqn 21}$$

where $<\kappa>_\tau = \kappa_o <e^{-E_r/kT}>_\tau$. Time-averaging of the fluxes is appropriate in equations 20–21 because residence times of labile soil C are typically measured in years to decades (Trumbore *et al.* 1996). Equation 20 links the storage, flux and turnover of soil C to the rate of biomass production by plants and the decomposition constant κ. Equation 21, in turn, links κ to the sizes, abundances and metabolic rates of decomposers ($\kappa_o = r_o^H M_{Tot}^H <M_H^{-1/4}>_M / S$). In equations 20–21, labile soil C and heterotroph biomass both decline with long-term temperature increases ($\propto <e^{-E_p/kT}>_\tau / <e^{-E_r/kT}>_\tau$) due to differences in the temperature dependence of photosynthesis and respiration. This, in turn, implies that the amount of decomposer biomass per unit labile soil C, $M_{Tot}^H <M_H^{-1/4}>_M / S$, is independent of temperature. Equations 20–21 also predict an increase in soil C and heterotroph biomass with increases in the fractional day-length, γ/τ, due to greater photosynthetic activity during the biologically active period of the year when temperatures exceed 0 °C.

Table 1. Predicted effects of average body size, $\langle M \rangle_J$, and average growing season temperature, $\langle T \rangle_\tau$, on long-term carbon flux, storage and turnover for the pools and fluxes depicted in Fig. 1

Pool	Variable (y)	Body size and temperature dependence	Predicted slope holding temperature or size constant	
			$\ln(y)$ *vs* $\ln(\langle M \rangle_J)$	$\ln(y)$ *vs* $1/k\langle T \rangle_\tau$
Autotrophs	Flux	$(\tau/\gamma)\langle n \rangle_\tau \propto \langle e^{-E_p/kT} \rangle_\tau \langle M_A \rangle_J^0$	0	$-E_p$
	Storage	$M_{Tot}^A \propto \langle e^{0/kT} \rangle_\tau / \langle M_A^{-1/4} \rangle_M$	1/4	0
	Turnover	$(\tau/\gamma)\langle n \rangle_\tau / M_{Tot}^A \propto \langle e^{-E_p/kT} \rangle_\tau \langle M_A^{-1/4} \rangle_M$	–1/4	$-E_p$
Heterotrophs	Flux	$(\tau/\gamma)\langle r_H \rangle_\tau = (\tau/\gamma)\langle n \rangle_\tau \propto \langle e^{-E_p/kT} \rangle_\tau \langle M_H \rangle_J^0$	0	$-E_p$
	Storage	$(\tau/\gamma) M_{Tot}^H \propto \langle e^{-E_p/kT} \rangle_\tau / \langle e^{-E_r/kT} \rangle_\tau \langle M_H^{-1/4} \rangle_J$	1/4	$E_r - E_p$
	Turnover	$\langle s \rangle_\tau / M_{Tot}^H \propto \langle r_H \rangle_\tau / M_{Tot}^H \propto \langle e^{-E_r/kT} \rangle_\tau \langle M_H^{-1/4} \rangle_M$	–1/4	$-E_r$
Labile soil	Flux	$(\tau/\gamma)\langle r_H \rangle_\tau \propto \langle e^{-E_p/kT} \rangle_\tau$	–	$-E_p$
organic matter	Storage	$(\tau/\gamma) S \propto \langle e^{-E_p/kT} \rangle_\tau / \langle e^{-E_r/kT} \rangle_\tau$	–	$E_r - E_p$
	Turnover	$\langle r_H \rangle_\tau / S \propto \langle e^{-E_r/kT} \rangle_\tau$	–	$-E_r$

Parameters include activation energy for ATP synthesis in the respiratory complex ($E_r \approx 0{\cdot}65$ eV); effective activation energy for Rubisco carboxylation in C_3 photosynthesis ($E_p \approx 0{\cdot}32$ eV, see Appendix 1); growing season length, τ, defined as the number of hours per year when average daily temperatures exceed 0 °C; and daylight hours during the growing season, γ.
Time-averaged fluxes, $\langle \rangle_\tau$, are calculated by averaging rates over the entire growing season. The predicted slopes involve the following approximations: $\langle e^{-E/kT} \rangle_\tau \approx e^{-E/k\langle T \rangle_\tau}$ and $\langle M^{-1/4} \rangle_M \approx \langle M \rangle_J^{-1/4}$, which can be justified using methods described by Savage (2004).

STEP 5: CHARACTERIZING ECOSYSTEM-LEVEL CO_2 FLUX

Equations 1–21 yield the following expression for whole-ecosystem respiration:

$$r_{Tot} = r_A + r_H = r_o^{Tot} e^{-E_r/kT} \qquad \text{eqn 22}$$

where $r_o^{Tot} = (\gamma/\tau) p_o M_{Tot}^A \langle M_A^{-1/4} \rangle_M (\langle e^{-E_p/kT} \rangle_\tau / \langle e^{-E_r/kT} \rangle_\tau)$. Equation 22 predicts a rapid increase in respiration with temperature at diurnal to seasonal time scales for autotrophs and heterotrophs ($\propto e^{-E_r/kT}$). However, it also predicts that respiration at a given temperature will decline if growing-season temperatures increase to some new, long-term average ($r_o^{Tot} \propto \langle e^{-E_p/kT} \rangle_\tau / \langle e^{-E_r/kT} \rangle_\tau$). Finally, it predicts that respiration at a given temperature will decline towards low latitudes as average day-lengths during the growing season shorten ($r_o^{Tot} \propto \gamma/\tau$). All these phenomena reflect the fact that photosynthesis, with its weaker temperature dependence ($E_p < E_r$), constrains whole-ecosystem CO_2 flux to equal GPP (Fig. 1). This constraint on CO_2 flux is manifested at the individual level for autotrophs through respiratory acclimation (equation 17), and at the community level for heterotrophic decomposers through changes in abundance, biomass and the size of the labile soil C pool (equations 20–21).

Evaluating model predictions

Equations 1–22 yield a series of testable, quantitative predictions on the size and temperature dependence of flux, storage and turnover within and among the C pools depicted in Fig. 1 (Table 1). We evaluate many of these predictions using global compilations of data from major biomes that include forests, grasslands, tundra and oceans. The predictions in Table 1 are derived by explicitly accounting for day-length and length of growing season. For example, NPP is expressed on a per daylight hour basis during the growing season, $(\tau/\gamma)\langle n \rangle_\tau$ (g C m^{-2} daylight h^{-1}); C storage in soil is corrected for average day-length, $(\tau/\gamma)S$ (g C m^{-2} h daylight h^{-1}); and C turnover in soil is expressed on a per hour basis during the growing season, $\langle r_H \rangle_\tau / S$ (h^{-1}). Where possible we evaluate long-term temperature predictions using these 'seasonality-corrected' values to control for latitudinal variation in day-length and length of growing season, which might otherwise confound the predicted temperature relationships.

Results

Data support the predicted size dependence of C storage and turnover in the autotroph pool (Table 1). First, a log–log plot of C storage in autotrophs *vs* average plant size yields a linear relationship with a slope of 0·24, which is statistically indistinguishable from the predicted value of 0·25 (95% CI: 0·23–0·26; Fig. 2a). Second, a log–log plot of C turnover *vs* average plant size yields a linear relationship with a slope of –0·22, which is just slightly shallower than the predicted value of –0·25 (95% CI: –0·21 to –0·24; Fig. 2b). Third, C flux is predicted to be independent of body size if resource use is at equilibrium with supply. The analysis of Enquist *et al*. (1998) supports this prediction by finding a slope close to the predicted value of 0 for plant communities spanning 12 orders of magnitude in average plant size.

The model makes additional predictions based on the temperature dependence of photosynthesis ($\propto e^{-E_p/kT}$) and respiration ($\propto e^{-E_r/kT}$) (Table 1). Carbon storage is predicted to be independent of temperature for the

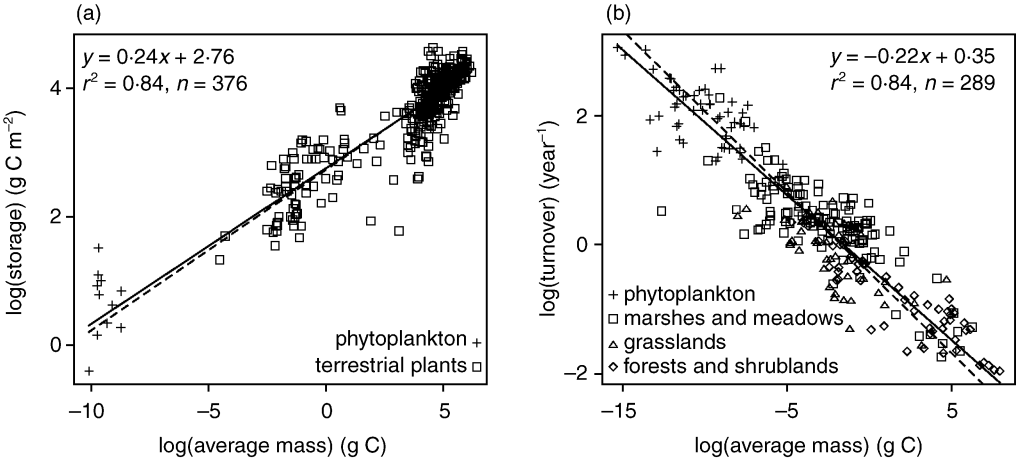

Fig. 2. Effects of body size on (a) carbon storage (compilation of woody, herbaceous and marine plant community data in Belgrano *et al.* 2002); (b) turnover in plant communities (compilation in Cebrian 1999). The slope in (a) was calculated using ordinary least-squares regression. (b) Body size was estimated from plant biomass using the data in (a). Reduced major-axis regression was then used to fit the slope in (b) to account for errors that this method of estimation introduced into the predictor variable. The fitted, solid lines have slopes close to the predicted, dashed lines with slopes of 0·25 (a) and –0·25 (b) (Table 1).

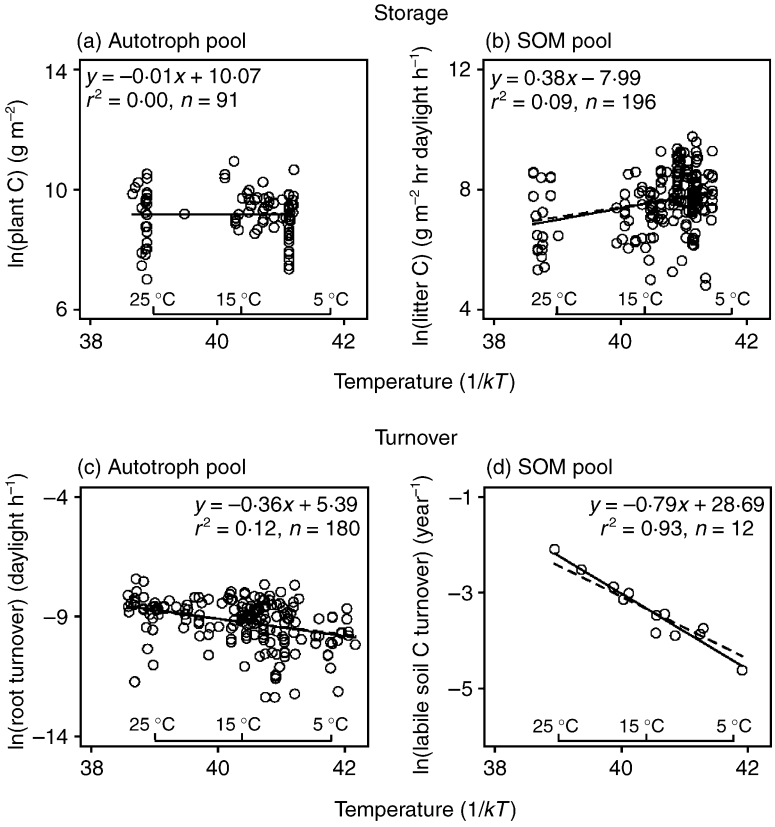

Fig. 3. Effect of average temperature, expressed as $1/k<T>_\tau$, on (a) forest tree biomass (global database in DeAngelis *et al.* 1997); (b) seasonality-corrected forest litter storage (global compilation in Vogt *et al.* 1986); (c) seasonality-corrected fine-root turnover (global compilation of shrubland, grassland and forest data in Gill & Jackson 2000); (d) soil organic matter (SOM) turnover (data from Fig. 2b of Trumbore *et al.* 1996). (a–c) Average growing season temperature, $<T>_\tau$ (K), and average growing season length, τ (h), were calculated based on months with average temperatures exceeding 0 °C using the database of Legates & Wilmott (1990). (d) Mean annual temperatures of Trumbore *et al.* (1996) were used. The number of daylight hours during the growing season, γ, was estimated using the equation of Forsythe *et al.* (1995). (a–c) Seasonality-corrected values were calculated using τ and γ (Table 1). Solid, fitted lines were calculated using ordinary least-squares regression. Predicted, dashed lines have slopes of 0 eV (a); $E_r - E_p = 0{\cdot}33$ eV (b); $-E_p = -0{\cdot}32$ eV (c); $-E_r = -0{\cdot}65$ eV (d) (Table 1).

autotroph pool because respiration and growth are constrained by photosynthesis at the level of the organism (equations 11 and 17). Carbon storage in heterotrophs and soil organic matter is predicted to decline with increasing temperature. This is because the sizes of these pools are determined by the balance between production and consumption, and consumption by heterotrophs increases more rapidly with temperature than does production by plants. Extensive data support model predictions for the autotroph and soil C pools. First, a plot of the logarithm of C storage in autotrophs *vs* $1/kT$ for forest tree communities yields a slope statistically indistinguishable from the predicted value of 0 eV (95% CI: –0·18 to 0·17; Fig. 3a). Second, a plot of the logarithm of seasonality-corrected labile C storage *vs* $1/kT$ for forest litter yields a linear relationship with a slope statistically indistinguishable from the predicted value of $E_r - E_p = 0{\cdot}33$ eV (0·38 eV, 95% CI: 0·21–0·56; Fig. 3b).

For both autotroph and heterotroph pools, C turnover varies with temperature in the same way as individual metabolic rate, because the fractions of metabolic energy allocated to growth (ε and δ in Fig. 1) are independent of temperature. For the soil C pool, turnover is controlled by heterotroph respiration. Carbon turnover is therefore predicted to show a weaker temperature dependence for the autotroph pool than for heterotrophs and soil C (Table 1). A plot of the logarithm of seasonality-corrected fine root turnover *vs* $1/kT$ yields a slope close to the predicted value of $-E_p = -0{\cdot}32$ eV for the autotroph pool (–0·36 eV; 95% CI: –0·22 to –0·51; Fig. 3c). However, a plot of the logarithm of labile C turnover in soil *vs* $1/kT$ yields a slope somewhat steeper than the predicted value of $-E_r = -0{\cdot}65$ eV (–0·79 eV, 95% CI: –0·66 to –0·93; Fig. 3d). This is perhaps because climatic data were not available to apply seasonality correction to the estimated temperatures and rates of C turnover.

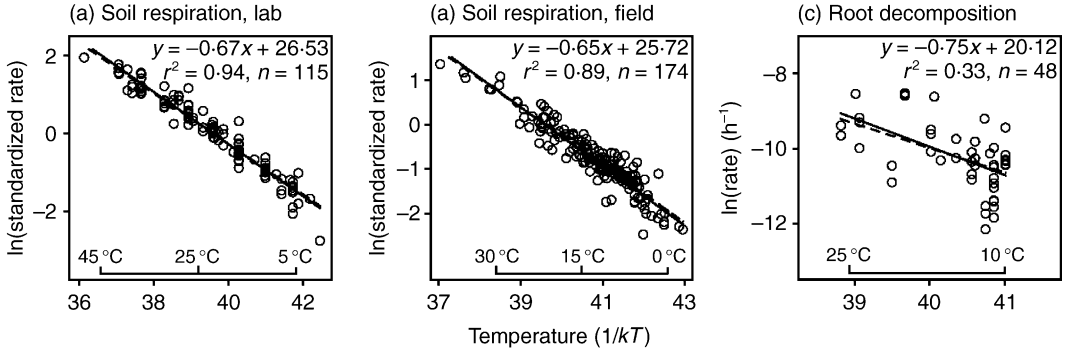

Fig. 4. Effect of temperature, expressed as $1/kT$, on the following short-term fluxes. (a) Standardized fluxes of CO_2 from soils incubated at different constant temperatures in the laboratory [compilation in Katterer *et al*. (1998) supplemented with data in Drobnik (1962); Wiant (1965); Mallik & Hu (1997); Quemada & Cabrera (1997); Chodak *et al*. (2001)]. (b) Standardized fluxes of CO_2 from soils measured over multiple seasons in the field [compilation in Lloyd & Taylor (1994) supplemented with data in Boone *et al*. (1998); Keith *et al*. (1997); Luo *et al*. (2001)]. Methods used to standardize the data in (a) and (b) are discussed in Appendix 1. (c) Hourly root decomposition rates in the growing season for sites spanning a broad range of latitudes (subset of studies compiled in Silver & Miya 2001). Average growing season temperature, $<T>_\tau$ (K), and average growing season length, τ (h), calculated based on months with average temperatures exceeding 0 °C using the database of Legates & Wilmott (1990). Solid, fitted lines calculated using ordinary least-squares regression. Predicted, dashed lines all have slopes of $-E_r = -0{\cdot}65$ eV (equations 16, 19 and 22).

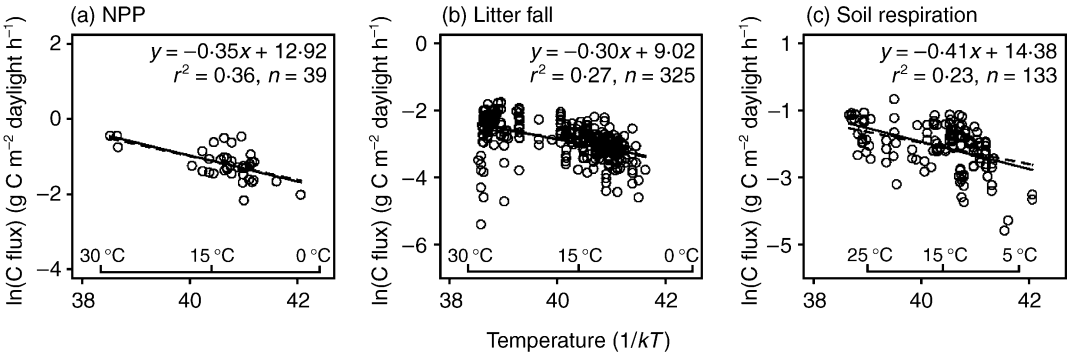

Fig. 5. Effect of average growing season temperature, expressed as $1/k<T>_\tau$, on the following long-term fluxes: (a) seasonality-corrected NPP (data used to fit the temperature relationship in the Miami model of Lieth 1973); (b) seasonality-corrected forest litter fall [compilations in Bray & Gorham (1964); Vitousek (1984)]; (c) seasonality-corrected soil respiration (compilation in Raich & Schlesinger 1992, excluding estimates based on some assumed growing season length). Average growing season temperature, $<T>_\tau$ (K), calculated using the database of Legates & Wilmott (1990) based on months with average temperatures exceeding 0 °C. The number of daylight hours during the growing season, γ, was then calculated using the equation of Forsythe *et al*. (1995). Seasonality-corrected values were calculated by dividing annual fluxes by γ (Table 1). Solid, fitted lines were calculated using ordinary least-squares regression. Predicted, dashed lines all have slopes of $-E_p = -0{\cdot}32$ eV (Table 1).

Our model predicts a much stronger temperature dependence for short-term respiratory fluxes, and for rates of organic matter decomposition (characterized by κ in equation 19), than for long-term respiratory fluxes. Consequently, respiratory fluxes at a given temperature are predicted to decline with long-term temperature increases (characterized by r_o^{Tot} in equation 22). Two compilations of data support the predicted temperature dependence of short-term flux, with slopes close to $-E_r = -0{\cdot}65$ eV: (i) laboratory data on heterotroph respiration rates from diverse soils (–0·67, 95% CI: –0·62 to –0·71; Fig. 4a), and (ii) field data on seasonal variation in CO_2 flux from soil heterotrophs and roots of forest, grassland and tundra autotrophs (–0·65, 95% CI: –0·60 to –0·70; Fig. 4b). A third compilation of data on root decomposition rates supports the predicted temperature dependence for κ, with a slope consistent with $-E_r = -0{\cdot}65$ eV (–0·75, 95% CI: –0·44 to –1·06; Fig. 4c).

Three additional global data sets support the predicted temperature dependence of long-term flux, with slopes statistically indistinguishable from $-E_p = -0{\cdot}32$ eV: (i) seasonality-corrected NPP (–0·35 eV, 95% CI: –0·20 to –0·50; Fig. 5a); (ii) seasonality-corrected litter fall (–0·30 eV, 95% CI: –0·24 to –0·35; Fig. 5b); and (iii) seasonality-corrected soil respiration (–0·41 eV, 95% CI: –0·28 to –0·54; Fig. 5c). Together, these results suggest that long-term ecosystem respiration rates are controlled primarily by the availability of organic C which, in turn, is controlled by the rate of photosynthesis.

The predicted relationship between short- and long-term flux is supported by a recent analysis of data collected from 19 eddy covariance towers in North America and Europe (Enquist *et al*. 2003). At individual

sites, daily and seasonal variation in CO_2 flux increased exponentially with temperature with an average activation energy close to E_r ($\bar{x} = 0{\cdot}62$ eV), but across sites, respiration rates at a given temperature (characterized by r_o^{Tot}) declined with increasing average growing season temperature, as predicted here by equation 22.

Discussion

The model presented here provides a means of characterizing the role of individual organisms in the global C cycle. Biota play key roles in the biogeochemical cycling of elements, but quantifying them explicitly is challenging (Jones & Lawton 1995). Our model quantifies these roles using three simplifying assumptions: (i) metabolic rate controls energy and material transformation rates by an organism; (ii) metabolic rate controls energy and material fluxes between an organism and its environment; and (iii) ecosystem storage and flux attributable to biota are equal to the sums of the storage and flux contributions of individual organisms. Assumptions (ii) and (iii) follow directly from (i) as a consequence of mass and energy balance, and link the cycling of elements in ecosystems to individual physiology.

The combined effects of body size and temperature on metabolic rate impose important constraints on C dynamics. Variation in C storage and turnover across biomes is driven largely by plant size (Fig. 2). Our model thus explains why oceanic phytoplankton contribute ≈50% of NPP globally despite comprising only 0·2% of the Earth's plant biomass (Field *et al*. 1998). Incorporating body size in C-cycling models could reveal other causes of variation in C dynamics across biomes. It could also predict the effects of land use on C dynamics, because land conversion often entails altering the size distribution of organisms, for example converting a forest to a field for agriculture.

The temperature dependence of many rate processes typically considered separately in ecosystem models falls into one of three categories: those controlled by photosynthesis; by respiration; or by a balance between photosynthesis and respiration. Long-term rates controlled by photosynthesis (e.g. NPP, litter fall, fine-root turnover, annual CO_2 flux from soils) all increase approximately fourfold from 0 to 30 °C (Figs 3c and 5), even after accounting for day-length and length of the growing season, and are predicted from the temperature dependence of Rubisco carboxylation (Appendix 1). These results challenge the idea that mean annual temperature and NPP are correlated, largely because temperature is an index of growing season length and incident solar radiation (Lieth 1973). Labile C turnover (Fig. 3d), organic matter decomposition, and short-term respiratory fluxes of CO_2 from autotrophs, heterotrophs and soils (Fig. 4) all increase approximately 16-fold from 0 to 30 °C, and are predicted from the activation energy of the respiratory complex ($E_r = 0{\cdot}65$ eV). Finally, three different phenomena – acclimation of plant respiration; geographic gradients in labile C storage; and differences between the short- and long-term temperature dependence of ecosystem CO_2 flux – are predicted from the different temperature dependencies of photosynthesis and respiration, reflecting constraints of photosynthate production on oxidative metabolism (equations 14, 17, 18 and 19).

More generally, our model predicts many aspects of the global C cycle based on the primary effects of body size and temperature on photosynthesis and respiration. We attribute the model's explanatory power to the explicit dependence of ecosystem-level C flux and storage on individual-level fluxes. We are aware, however, that there is considerable residual variation about the relationships depicted in Figs 2–5. This variability points to the importance of other variables that affect C cycling, including water, light and nutrient availability (Lieth 1973; Vitousek 1984; Field *et al*. 1998; Schimel *et al*. 2001; Chapin *et al*. 2002). Deviations from model predictions reflect these other variables. Consider the following two examples. First, residual variation about the function describing the temperature dependence of root decomposition (Fig. 4c) is strongly correlated with the root C : N ratio ($r^2 = 0{\cdot}65$, $P < 0{\cdot}01$). This residual variation reflects the influence of resource quality and nutrient availability on the normalization parameter for organic matter decomposition (κ_o in equation 19) which, in turn, reflects the sizes, abundances and metabolic rates of heterotrophic decomposers in soils (equation 21); and second, a global compilation of data on C storage in mineral soils (Zinke *et al*. 1984) yields a relationship between seasonality-corrected soil C and temperature that is much weaker than predicted by our model under the assumption that all organic matter is labile C accessible to heterotrophs (predicted slope: $E_r - E_p = 0{\cdot}33$ eV; observed slope: 0·11 eV, 95% CI: 0·08–0·14 eV, $r^2 = 0{\cdot}01$, $n = 4023$). This supports evidence that much of the organic matter stored in mineral soils is inaccessible to heterotrophs, and therefore is not susceptible to the effects of global warming (Thornley & Cannell 2001). The model could be extended to incorporate the buildup of refractory C in soil.

Our model is relevant for understanding and predicting the effects of human activities on the C cycle at local to global scales. For example, it predicts ecosystem responses to global warming. While it does not predict the total size of the global fluxes and pools, it does predict that global warming should increase rates of photosynthesis and respiration. It also predicts that increases in temperature will cause a net loss of labile C from soils. The magnitude of this loss is controlled by the difference between the temperature dependence of respiration and Rubisco carboxylation ($E_r - E_p$). A sustained 1 °C increase in average growing season temperature should therefore result in approximately fourfold greater losses of labile C from boreal forest soils ($<T>_\tau = 0$ °C) than from tropical forest soils ($<T>_\tau = 25$ °C) (equation 21). We caution, however, that

these predictions ignore possible short-term transient dynamics, and they assume that other variables, including atmospheric CO_2 concentration and water and nutrient availability, are held constant.

In summary, the model presented here makes multiple predictions (Table 1), many of which are supported by previous studies (e.g. Kirschbaum 2000) or by compilations of data from the literature (Figs 2–5). However, unlike previous work, this simple, mechanistic model yields predictions by quantifying the combined effects of two key variables, body size and temperature, on biologically controlled components of the global C cycle. It does so by linking the pools and fluxes of C in ecosystems directly to the metabolic rates of individual organisms that proximally and ultimately control C dynamics.

Acknowledgements

We thank G.B. West, V.M. Savage, B.T. Milne, S.L. Collins, H. Olff, and two anonymous reviewers for comments. J. Lloyd and T. Katterer generously provided data. A.P.A. is grateful for the support of the NSF. J.F.G. and J.H.B. are grateful for the support of the Thaw Charitable Trust and a Packard Interdisciplinary Science Grant.

References

Belgrano, A., Allen, A.P., Enquist, B.J. & Gillooly, J.F. (2002) Allometric scaling of maximum population density: a common rule for marine phytoplankton and terrestrial plants. *Ecology Letters* **5**, 611–613.

Bernacchi, C.J., Singsaas, E.L., Pimentel, C., Portis, A.R. & Long, S.P. (2001) Improved temperature response functions for models of Rubisco-limited photosynthesis. *Plant, Cell & Environment* **24**, 253–259.

Boone, R.D., Nadelhoffer, K.J., Canary, J.D. & Kaye, J.P. (1998) Roots exert a strong influence on the temperature sensitivity of soil respiration. *Nature* **396**, 570–572.

Bray, J.R. & Gorham, E. (1964) Litter production in forests of the world. *Advances in Ecological Research* **2**, 101–157.

Brown, J.H., Gillooly, J.F., Allen, A.P., Savage, V.M. & West, G.B. (2004) Toward a metabolic theory of ecology. *Ecology* **85**, 1771–1789.

Cebrian, J. (1999) Patterns in the fate of production in plant communities. *American Naturalist* **154**, 449–468.

Chapin, F.S., Matson, P.A. & Mooney, H.A. (2002) *Principles of Ecosystem Ecology*. Springer-Verlag, New York.

Chodak, M., Borken, W., Ludwig, B. & Beese, F. (2001) Effect of temperature on the mineralization of C and N of fresh and mature compost in sandy material. *Journal of Plant Nutrition and Soil Science* **164**, 289–294.

DeAngelis, D.L., Gardner, R.H. & Shugart, H.H. (1997) *Productivity of forest ecosystems studied during the IBP: the woodlands data set*. Oak Ridge National Laboratory Archive Center, Oak Ridge, TN, USA. www.daac.ornl.gov

Dewar, R.C., Medlyn, B.E. & McMurtrie, R.E. (1999) Acclimation of the respiration photosynthesis ratio to temperature: insights from a model. *Global Change Biology* **5**, 615–622.

Drobnik, J. (1962) The effect of temperature on soil respiration. *Folia Microbiologica* **7**, 132–140.

Else, P.L. & Hulbert, A.J. (1985) Mammals: an allometric study of metabolism at tissue and mitochondrial level. *American Journal of Physiology* **248**, R415–R421.

Enquist, B.J., Brown, J.H. & West, G.B. (1998) Allometric scaling of plant energetics and population density. *Nature* **395**, 163–165.

Enquist, B.J., Economo, E.P., Huxman, T.E., Allen, A.P., Ignace, D.D. & Gillooly, J.F. (2003) Scaling metabolism from organisms to ecosystems. *Nature* **423**, 639–642.

Farquhar, G.D., von Caemmerer, S. & Berry, J.A. (1980) A biochemical model of photosynthetic CO_2 assimilation in leaves of C_3 plants. *Planta* **149**, 78–90.

Field, C.B., Behrenfeld, M.J., Randerson, J.T. & Falkowski, P. (1998) Primary production of the biosphere: integrating terrestrial and oceanic components. *Science* **281**, 237–240.

Forsythe, W.C., Rykiel, E.J., Stahl, R.S., Wu, H.I. & Schoolfield, R.M. (1995) A model comparison for daylength as a function of latitude and day of year. *Ecological Modelling* **80**, 87–95.

Gallardo, A. & Schlesinger, W.H. (1994) Factors limiting microbial biomass in the mineral soil and forest floor of a warm-temperate forest. *Soil Biology and Biochemistry* **26**, 1409–1415.

Gifford, R.M. (2003) Plant respiration in productivity models: conceptualisation, representation and issues for global terrestrial carbon-cycle research. *Functional Plant Biology* **30**, 171–186.

Gill, R.A. & Jackson, R.B. (2000) Global patterns of root turnover for terrestrial ecosystems. *New Phytologist* **147**, 13–31.

Gillooly, J.F., Brown, J.H., West, G.B., Savage, V.M. & Charnov, E.L. (2001) Effects of size and temperature on metabolic rate. *Science* **293**, 2248–2251.

del Giorgio, P.A. & Cole, J.J. (1998) Bacterial growth efficiency in natural aquatic systems. *Annual Review of Ecology and Systematics* **29**, 503–541.

Jenkinson, D.S. (1990) The turnover of organic carbon and nitrogen in soil. *Philosophical Transactions: Biological Sciences* **329**, 361–367.

Jones, C.G. & Lawton, J.H. (1995) *Linking Species and Ecosystems*. Chapman & Hall, New York.

Katterer, T., Reichstein, M., Andren, O. & Lomander, A. (1998) Temperature dependence of organic matter decomposition: a critical review using literature data analyzed with different models. *Biology and Fertility of Soils* **27**, 258–262.

Keith, H., Jacobsen, K.L. & Raison, R.J. (1997) Effects of soil phosphorus availability, temperature and moisture on soil respiration in *Eucalyptus pauciflora* forest. *Plant and Soil* **190**, 127–141.

Ketchum, C.J. & Nakamoto, R.K. (1998) A mutation in the *Escherichia coli* F0F1-ATP synthase rotor, gamma E208K, perturbs conformational coupling between transport and catalysis. *Journal of Biological Chemistry* **28**, 22292–22297.

Kirschbaum, M.U.F. (2000) Will changes in soil organic carbon act as a positive or negative feedback on global warming? *Biogeochemistry* **48**, 21–51.

Legates, D.R. & Wilmott, C.J. (1990) Mean seasonal and spatial variability in global surface air temperature. *Theoretical and Applied Climatology* **41**, 11–21.

Lieth, H. (1973) Primary production: terrestrial ecosystems. *Human Ecology* **1**, 303–332.

Lloyd, J. & Taylor, J.A. (1994) On the temperature-dependence of soil respiration. *Functional Ecology* **8**, 315–323.

Long, S.P. & Hutchin, P.R. (1991) Primary production in grasslands and coniferous forests with climate change – an overview. *Ecological Applications* **1**, 139–156.

Luo, Y.Q., Wan, S.Q., Hui, D.F. & Wallace, L.L. (2001) Acclimatization of soil respiration to warming in a tall grass prairie. *Nature* **413**, 622–625.

Mallik, A.U. & Hu, D. (1997) Soil respiration following site preparation treatments in boreal mixed wood forest. *Forest Ecology and Management* **97**, 265–275.

Niklas, K.J. & Enquist, B.J. (2001) Invariant scaling relationships for interspecific plant biomass production rates and body size. *Proceedings of the National Academy of Sciences, USA* **98**, 2922–2927.

Quemada, M. & Cabrera, M.L. (1997) Temperature and moisture effects on C and N mineralization from surface applied clover residue. *Plant and Soil* **189**, 127–137.

Raich, J.W. & Schlesinger, W.H. (1992) The global carbon dioxide flux in soil respiration and its relationship to vegetation and climate. *Tellus Series B – Chemical and Physical Meteorology* **44**, 81–99.

Savage, V.M. (2004) Improved approximations to scaling relationships for species, populations, and ecosystems across latitudinal and elevational gradients. *Journal of Theoretical Biology* **227**, 525–534.

Savage, V.M., Gillooly, J.F., Brown, J.H., West, G.B. & Charnov, E.L. (2004) Effects of body size and temperature on population growth. *American Naturalist* **163**, E429–E441.

Schimel, D.S., House, J.I., Hibbard, K.A. *et al.* (2001) Recent patterns and mechanisms of carbon exchange by terrestrial ecosystems. *Nature* **414**, 169–172.

Schlesinger, W.H. (1990) Evidence from chronosequence studies for a low carbon-storage potential of soils. *Nature* **348**, 232–234.

Schlesinger, W.H. (1997) *Biogeochemistry: an Analysis of Global Change*. Academic Press, San Diego, CA, USA.

Silver, W.L. & Miya, R.K. (2001) Global patterns in root decomposition: comparisons of climate and litter quality effects. *Oecologia* **129**, 407–419.

Thornley, J.H.M. & Cannell, M.G.R. (2001) Soil carbon storage response to temperature: an hypothesis. *Annals of Botany* **87**, 591–598.

Trumbore, S.E., Chadwick, O.A. & Amundson, R. (1996) Rapid exchange between soil carbon and atmospheric carbon dioxide driven by temperature change. *Science* **272**, 393–396.

Vitousek, P.M. (1984) Litterfall, nutrient cycling, and nutrient limitation in tropical forests. *Ecology* **65**, 285–298.

Vogt, K.A., Grier, C.C. & Vogt, D.J. (1986) Production, turnover, and nutrient dynamics of above- and belowground detritus of world forests. *Advances in Ecological Research* Vol. 15 (eds A. MacFadyen & E.D. Ford), pp. 303–377. Academic Press, New York.

West, G.B., Brown, J.H. & Enquist, B.J. (1997) A general model for the origin of allometric scaling laws in biology. *Science* **276**, 122–126.

West, G.B., Woodruff, W.H. & Brown, J.H. (2002) Allometric scaling of metabolic rate from molecules and mitochondria to cells and mammals. *Proceedings of the National Academy of Sciences, USA* **99**, 2473–2478.

Wiant, H.V. (1965) Influence of temperature on the rate of soil respiration. *Journal of Forestry* **65**, 489–490.

Zinke, P.J., Strangenberger, A.G., Post, W.M., Emanuel, W.R. & Olson, J.S. (1984) *Wordwide Organic Soil Carbon and Nitrogen Data*. Report no. ORNL/TM-8857. Oak Ridge National Laboratory, Oak Ridge, TN, USA.

Received 26 August 2004; revised 16 November 2004; accepted 29 November 2004

Appendix 1

APPROXIMATION FOR THE TEMPERATURE DEPENDENCE OF PHOTOSYNTHESIS

We approximate the temperature dependence of photosynthesis based on the biochemical kinetics of the C_3 photosynthetic pathway because it is the dominant photosynthetic pathway in the biosphere. The rate of C_3 photosynthesis can be limited by the availability of Rubisco to catalyse the carboxylation reaction, or by the light-dependent rate of RuBP regeneration (Farquhar *et al*. 1980). We hypothesize that the temperature dependence of C_3 photosynthesis can be approximated by the temperature dependence of Rubisco carboxylation, because theory and data indicate that photosynthesis is a rapidly saturating function of irradiance, and that leaf nitrogen is allocated among enzymes such that the Rubisco carboxylation step and the RuBP regeneration step are approximately colimiting (Chapin *et al*. 2002; Farquhar *et al*. 1980).

If Rubisco availability limits or colimits the carboxylation reaction, the rate of photosynthesis by a chloroplast is equal to:

$$v'_{chlo} = \frac{(1-\phi/2)}{1+(K_c/C)(1+O/K_o)} V_c^{\max} = \frac{(1-\phi/2)}{1+(K_c/C)(1+O/K_o)} v'_o e^{-E_c/kT} \quad \text{eqn A1}$$

The parameter $V_c^{\max} = v'_o e^{-E_c/kT}$ is the maximum rate of Rubisco carboxylation per chloroplast; K_c and K_o are the respective Michaelis–Menten constants for CO_2 and O_2; C and O are the respective partial pressures of CO_2 and O_2; ϕ is the ratio of Rubisco oxygenation (photorespiration) to carboxylation $\{\phi = [(V_o^{\max} K_c O)/(V_c^{\max} K_o C)]\}$; and $V_o^{\max}$ is the maximum rate of oxygenation (Farquhar *et al*. 1980). The parameters , $V_c^{\max}$, $V_o^{\max}$, K_c and K_o all increase exponentially with temperature, and can be described by Boltzmann factors of the form $e^{-E_i/kT}$, where E_i is an activation energy that varies from 0·37 eV for K_o to 0·83 eV for K_c (Bernacchi *et al*. 2001). So, for example, since $V_c^{\max} \propto e^{-E_c/kT}$ in equation A1, and E_c = 0·68 eV (Bernacchi *et al*. 2001), $V_c^{\max}$ increases 17·5-fold from 273 to 303 K (0–30 °C) ($e^{-E_c/303k}/e^{-E_c/273k} = 17{\cdot}5$).

The overall effect of temperature on v'_{chlo} is much weaker than on $V_c^{\max}$, primarily because the ratio of Rubisco carboxylation to photorespiration (characterized by ϕ in equation A1) declines markedly with increasing temperature. Using the parameter estimates reported by Bernacchi *et al*. (2001) for the temperature dependence of Rubisco carboxylation, and assuming that the partial pressure of CO_2 inside the chloroplast stroma is maintained at ≈70% of ambient pressures (Long & Hutchin 1991) (C = 0·028% on a molar basis in equation A1), v'_{chlo} is predicted to increase only 3·8-fold from 0 to 30 °C under present partial pressures of CO_2 and O_2. For a rate process exhibiting Boltzmann temperature dependence, this would correspond to an activation energy of E_p = 0·32 eV [$E_p = k \ln(3{\cdot}8)/(1/303 - 1/273)$]. We therefore approximate the temperature dependence of photosynthesis using a Boltzmann relationship with this same activation energy ($v'_{chlo} \approx v_{chlo} = v_o^{chlo} e^{-E_p/kT}$), where v_o^{chlo} is a normalization

parameter independent of plant size and temperature (g C chloroplast^{-1} daylight h^{-1}). This is a reasonable approximation over the temperature range 0–30 °C ($\ln(v'_{chlo}) = -E_p(1/kT) + \ln(v_o^{chlo})$, $r^2 = 0{\cdot}96$).

METHOD OF DATA STANDARDIZATION IN FIGURE 4

Standardization was performed by separately submitting all the data in Fig. 4 to analysis of covariance (ANCOVA) to determine the functional relationship between soil flux, q, and temperature, $1/kT$ [$\ln(q) = -E(1/kT) + C$]. ANCOVA yielded an overall estimate of the activation energy, E, and a set of intercepts, C, that varied by study. E and C were then used to calculate estimates of soil flux at 20 °C, $q(20)$, for each study. Finally, flux data for each study were separately standardized by their respective flux estimates, $q(T)/q(20)$, to control for variation in C. Others have performed data standardization by separately fitting models to data from each study to calculate $q(20)$ (e.g. Lloyd & Taylor 1994). However, using this alternative approach, the overall temperature dependence can vary depending on the temperature used for standardization.